



Changes in choriocapillaris structure occurring in idiopathic macular hole before and after vitrectomy

Hiroaki Endo¹ · Satoru Kase² · Mitsuo Takahashi¹ · Yuki Ito¹ · Shozo Sonoda³ · Tomonori Sakoguchi³ · Taiji Sakamoto³ · Satoshi Katsuta¹ · Susumu Ishida² · Manabu Kase¹

Received: 17 November 2022 / Revised: 16 January 2023 / Accepted: 2 February 2023 / Published online: 16 February 2023
© The Author(s), under exclusive licence to Springer-Verlag GmbH Germany, part of Springer Nature 2023

Abstract

Purpose The aim of this study was to analyze the anatomical choroidal vascular layers and the changes in idiopathic macular hole (IMH) eyes over time after vitrectomy.

Methods This is a retrospective observational case–control study. Fifteen eyes from 15 patients who received vitrectomy for IMH and age-matched 15 eyes from 15 healthy controls were enrolled in this study. Retinal and choroidal structures were quantitatively analyzed before vitrectomy and 1 and 2 months after surgery using spectral domain-optical coherence tomography. Each choroidal vascular layer was divided into the choriocapillaris, Sattler's layer, and Haller's layer, and then, the choroidal area (CA), luminal area (LA), stromal area (SA), and central choroidal thickness (CCT) were calculated using binarization techniques. The ratio of LA to CA was defined as the L/C ratio.

Results The CA, LA, and L/C ratios were 36.9 ± 6.2 , 23.4 ± 5.0 , and 63.1 ± 7.2 in the choriocapillaris of IMH and were 47.3 ± 6.6 , 38.3 ± 5.6 , and 80.9 ± 4.1 in that of control eyes, respectively. Those values were significantly lower in IMH eyes than in control eyes (each $P < 0.01$), whereas there was no significant difference in total choroid, Sattler's layer, and Haller's layer or CCT. The ellipsoid zone defect length showed a significant negative correlation with the L/C ratio in total choroid and with CA and LA in the choriocapillaris of IMH ($R = -0.61$, $P < 0.05$, $R = -0.77$, $P < 0.01$, and $R = -0.71$, $P < 0.01$, respectively). In the choriocapillaris, the LA were 23.4 ± 5.0 , 27.7 ± 3.8 , and 30.9 ± 4.4 , and the L/C ratios were 63.1 ± 7.2 , 74.3 ± 6.4 , and 76.6 ± 5.4 at baseline, 1 month, and 2 months after vitrectomy, respectively. Those values showed a significant increase over time after surgery (each $P < 0.05$), whereas the other choroidal layers did not alter consistently with respect to changes in choroidal structure.

Conclusions The current OCT-based study demonstrated that the choriocapillaris was exclusively disrupted between choroidal vascular structures in IMH, which may correlate with the ellipsoid zone defect. Furthermore, the L/C ratio of choriocapillaris recovered after IMH repair, suggesting an improved balance between supply and demand of oxygen that has collapsed due to temporary loss of central retinal function by IMH.

Key messages

- It is known that the blood flow in the choriocapillaris could alter following macular hole surgery; however, little is known about the choroidal structure of macular hole eyes before and after vitrectomy by segmenting the choroidal vascular layers.
- This study highlighted that the ratio of luminal area in total choroidal area was lower in eyes with idiopathic macular hole than in control eyes in the choriocapillaris by segmenting three vascular sublayers using a new binarization technique.
- In the choriocapillaris, the luminal area and the ratio of luminal area in total choroidal area showed a significant increase over time after vitrectomy in macular hole eyes.

✉ Satoru Kase
kaseron@med.hokudai.ac.jp

¹ Department of Ophthalmology, Teine Keijinkai Hospital, Sapporo, Japan

² Department of Ophthalmology, Faculty of Medicine and Graduate School of Medicine, Hokkaido University, N-15, W-7, Kita-Ku, Sapporo 060-8638, Japan

³ Department of Ophthalmology, Kagoshima University, Kagoshima, Japan

Keywords Idiopathic macular hole · Optical coherence tomography · Choroidal structure · Choriocapillaris · L/C ratio

Introduction

Idiopathic macular hole (IMH) is the most common type of macular hole (MH), characterized by a defect in the retinal neuroepithelial tissue of the fovea [1, 2]. It is indisputable that vitreo-retinal interface abnormality and their traction play a major role in the development of MH. However, the exact pathophysiology underlying the development of IMH is unknown.

Previous studies have shown that anatomical and physiological changes in the choroid, an important metabolic source of the macula, may be associated with the progression of the MH. Aras et al. found that the foveal choriocapillaris blood flow and velocity were significantly reduced in the IMH eyes compared with the healthy eyes [3]. Zhang et al. also concluded that the choroidal thickness of the IMH eyes was significantly thinner than that of the contralateral eyes and reported that alterations of the choroidal thickness play a potential role in the pathogenesis of MH [4]. These findings suggest that choroidal morphological changes are involved as a cause or result of IMH formation, in which the traction mechanism proposed by Gass et al. might underlie [1, 2].

Optical coherence tomography (OCT) imaging has contributed to various clinical studies in the last few years, with enhanced depth imaging (EDI)-OCT and swept-source (SS)-OCT providing detailed choroidal structures [5]. Sonoda et al. [6] and Agrawal et al. [7] developed a binarization method for OCT images and proposed a new method to separate the whole choroid imaging into luminal and stromal components, which led to the evaluation individually and quantitatively. The OCT-based binarization has proved that the choroid played a critical role in the pathophysiology of various eye diseases such as central serous chorioretinopathy [8], polypoidal choroidal vasculopathy [9], myopic choroidal neovascularization [10], and diabetic retinopathy [11–13], branch retinal vein occlusion [14], Vogt-Koyanagi-Harada disease [15], and retinitis pigmentosa [16]. Furthermore, recent studies have suggested that the choroidal structure may change before and after surgery for full-thickness MH [17]. More recently, Sonoda et al. developed a new software called Eye Ground [18] and Kago-Eye2 [19] allowing the choroid to be semi-automatically segmented in binarized images. The choroid is a network of blood vessels and stromal tissue, composed of three layers: choriocapillaris, Sattler's layer, and Haller's layer. The inner and outer layers of the choroid have been reported to be differentially affected by various types of retinochoroidal disease [8, 19–21].

However, there are no studies that evaluate the choroidal structure of the IMH eye before and after vitrectomy by segmenting the three layers.

In this study, the aim was to analyze the anatomical choroidal vascular layers and to investigate the changes in IMH eyes over time after vitrectomy.

Methods

Ethics statement

This was a series of retrospective case series conducted at Teine Keijinkai Hospital. The procedure was approved by the Institutional Review Board (IRB) of Teine Keijinkai Hospital (IRB number: 2–021372-00) and followed the principles of the Declaration of Helsinki. Information about the purpose and protocol of the study was disclosed on the official website (http://www.keijinkai.com/teine/wpadmin/wp-content/uploads/2022/02/9_OPT2-021372-00.pdf), further guaranteeing the opportunity to refuse as much as possible for participants.

Study participants

We investigated IMH patients who visited the Retinal Vitreous Center of the Department of Ophthalmology, Teine Keijinkai Hospital, from June 2019 to August 2021. All eyes underwent comprehensive eye examinations, including visual acuity, intraocular pressure, slit-lamp microscopy of the anterior segment, and ophthalmoscopy of the fundus. The study selection criteria were set as follows: (1) 18 years and older at age; (2) idiopathic macular hole including small-medium size ($< 400 \mu\text{m}$) and large size ($> 400 \mu\text{m}$); (3) treatment by phacovitrectomy; and (4) 2-month follow-up after surgery. The exclusion criteria are (1) patients with diabetes and uncontrolled hypertension; (2) secondary or traumatic MH; (3) high myopia (refractive error > -6 diopter and/or axial length > 26 mm); (4) eyes with opacity of the transparent media which affects the image quality of OCT; and (5) glaucoma, trauma, uveitis, history of other retinal disorders, and prior ocular surgical interventions. Patient information was reviewed by electronic medical records: subjective visual symptoms and duration; best-corrected visual acuity (BCVA, logMAR) preoperatively and 1 and 2 months postoperatively; and

surgical techniques (PPV only; combined with cataract surgery). Stage of MH was determined according to both clinical features and intraoperative observations. The healthy control group was obtained from the OCT database of Teine Keijinkai Hospital, and the age, gender, refractive error, and axial length were matched with the IMH group.

OCT image acquisition

OCT images were acquired using spectral domain-OCT devices (Cirrus HD-OCT, Carl Zeiss Meditec, Dublin, CA). A horizontal raster scan pattern was used to perform a macular scan with a scan line of 9 mm centered on the fovea. OCT was performed between 9:00 AM and 11:00 AM to avoid diurnal variations. These were acquired by experienced technicians and evaluated for images with a signal strength of 7/10 or higher. In addition, OCT images were exported as a TIFF format for analysis with Kago-Eye2 software [19]. Each measurement was independently evaluated by two masked investigators (H.E. and Y.I.).

Retinal image analysis using OCT images

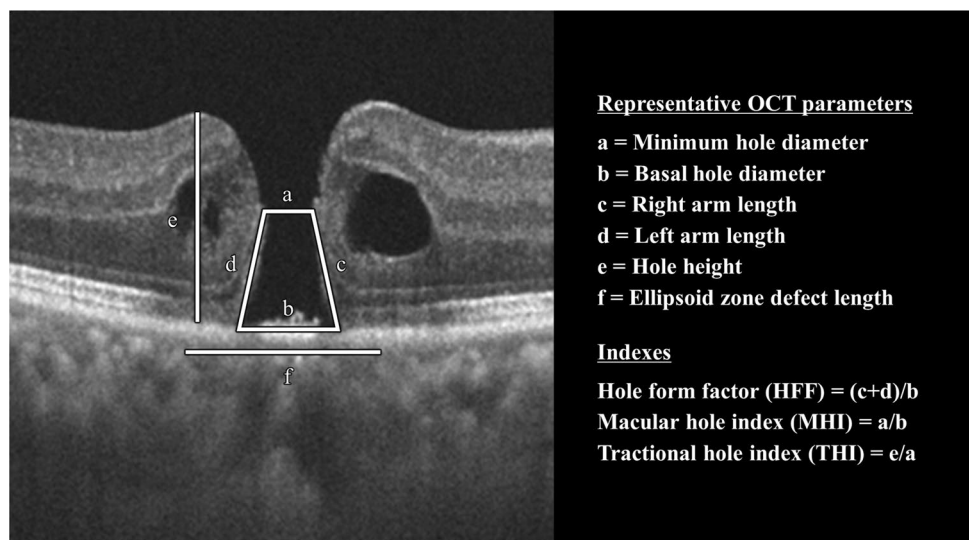
Using OCT images taken before surgery, minimum hole diameter, basal hole diameter, arm length, hole height, and EZ defect length were measured, and hole form factor (HFF), macular hole index (MHI), and tractional hole index (THI) were calculated as previously reported (Fig. 1) [22–24]. Minimum hole diameter was measured as the minimum distance between the inner edges of MH at the inner retinal layer level (Fig. 1a). Basal hole diameter was defined as MH diameter at the retinal pigment epithelium (RPE) level (Fig. 1b). Arm length corresponds to the distance connecting both ends of basal hole and minimum hole diameters (Fig. 1c and d). The hole height was considered the

maximum distance between the RPE and the vitreous retinal interface (Fig. 1e). The ellipsoid zone (EZ) defect length was extracted as the horizontal distance where the hyperreflective signal was lost (Fig. 1f). HFF is the quotient of the sum of the left and right arm lengths divided by the basal hole diameter and is the first OCT index known as a prognostic factor [22]. MHI is defined as the ratio of minimum hole diameter to basal hole diameter, which indicates tangential and anterior–posterior vitreomacular traction (VMT) or retinal hydration that is thought to act on the fovea to develop the macular hole. THI is defined as a ratio of the hole height to minimum hole diameter and represents the two traction forces responsible for macular holes, indicating the ratio of anterior–posterior vitreous traction and/or retinal hydration to tangential traction.

Choroidal image analysis using OCT images

The choroidal structure was analyzed using the established binarization technology [18, 19]. Figure 2 shows a representative image of the binarization of the choroid. The method is described in detail in a previous report [18, 19]. Briefly, after incorporating EDI-OCT images into the Kago-eye2 software, a 1500- μm wide choroidal region centered on the fovea was identified (Fig. 2A). After the evaluator determined the choroidal boundaries, semi-automatic segmentation was performed between the choriocapillaris and Sattler's layers and between the Sattler's and Haller's layers (Fig. 2B). Finally, OCT images of the choroidal region were binarized and choroidal area (CA), luminal area (LA), stromal area (SA), and central choroidal thickness (CCT) and were automatically measured (Fig. 2C, D). Bright and dark pixels corresponded to SA and LA, respectively (Fig. 2D). The ratio of LA to CA was defined as the L/C ratio.

Fig. 1 Parameter measurement and index calculation of optical coherence tomography in idiopathic macular hole (IMH). Optical coherence tomography (OCT) image of IMH showing **a** minimum hole diameter, **b** basal hole diameter, **c** right arm length, **d** left arm length, **e** hole height, and **f** ellipsoid zone defect length as measured by OCT. OCT indexes (hole form factor, macular hole index, tractional hole index) of various macular holes calculated by OCT parameters



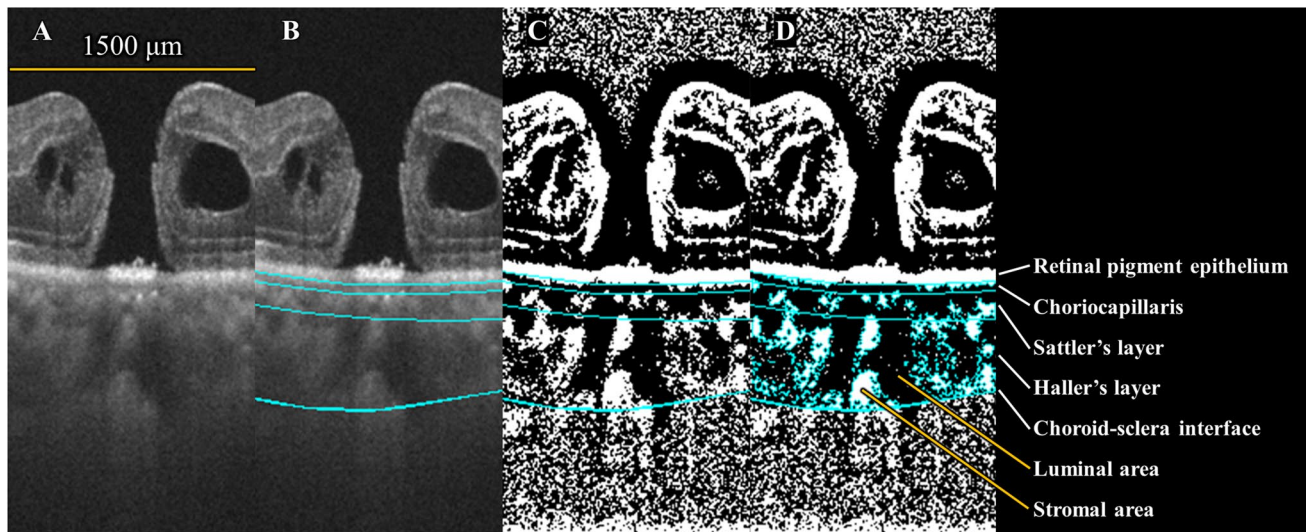


Fig. 2 Choroidal images of idiopathic macular hole (IMH) segmented by semi-automated software. **A** Preoperative enhanced depth imaging (EDI) optical coherence tomography (OCT) image of IMH. **B** Light blue lines indicate the retinal pigment epithelium-choriocapillaris interface, choriocapillaris-Sattler's border, Sattler's-Haller's

border, and choroid-sclera interface from the top. **C** EDI-OCT image converted to binarization by the Niblack method. Dark pixels were defined as luminal area and bright pixels as stromal area. **D** Total choroidal area, luminal area, and stromal area are calculated separately

Surgical procedure

All eyes underwent standard 25-gauge 3-port pars plana vitrectomy (PPV) combined with cataract surgery using the Constellation Vision System (Alcon Laboratories Inc., Fort Worth, TX, USA). Core vitrectomy was performed, and a posterior vitreous detachment was created as needed. Brilliant Blue G was used to stain and peel the internal limiting membrane (ILM). Finally, a fluid-air exchange was performed, followed by a replacement by sulfur hexafluoride (SF₆) into the vitreous cavity. The patients were instructed to maintain a prone position until a closure of the MH was confirmed with OCT following the surgery.

Statistical analysis

Statistical analysis was performed using commercially available statistical software SPSS version 21 (IBM Corporation, Chicago, USA). All data were expressed as mean \pm standard deviation. The chi-square test was used to compare the categorical variables. The Mann-Whitney *U* test was used to compare differences in various characteristics between IMH patients and controls. Spearman's rank correlation coefficient was used to investigate the relationship between the retina and choroidal structure in the IMH eyes. Changes in visual acuity and choroidal structure before and after surgery were analyzed using the Friedman test and Scheffe's paired comparison. *P* values below 0.05 were considered to be statistically significant.

Result

Demographics

Forty-one eyes were initially enrolled based on an IRB-approved study protocol. Twenty-six eyes, however, were excluded because the follow-up period was less than 2 months after surgery in 14 eyes; reliable OCT data were missing in 10 eyes; and diabetes mellitus in the systemic history was apparent in 2 eyes. Therefore, 15 eyes were eligible in this study. Fifteen eyes from 15 patients who received standard PPV for IMH and 15 eyes from 15 healthy controls were enrolled in this study. Table 1 shows the demographic factors and initial findings of the patients. There were no significant differences in age, gender, intraocular pressure, refractive power, axial length, hypertensive population, SBP, or DBP between healthy controls and IMH. The preoperative MH stage was stage 2 in 4 eyes (26.7%), stage 3 in 7 eyes (46.7%), and stage 4 in 4 eyes (26.7%). BCVA was significantly unfavorable in IMH eyes compared to healthy controls. The preoperative minimum hole diameter, basal hole diameter, hole height, and EZ defect length were 311 ± 144 , 676 ± 178 , 434 ± 92 , and 1383 ± 409 μ m, respectively. Preoperative HFF, MHI, and THI were 0.77 ± 0.16 , 0.77 ± 0.38 , and 1.50 ± 0.51 , respectively.

Reproducibility assessment of choroidal structural parameters

As shown in Table 2, the reliability of choroidal structure measurements in control and IMH eyes is tested. The intraclass

Table 1 Clinical and retinal characteristics of control and preoperative IMH eyes

	Control eyes	IMH eyes	<i>P</i> value
Number of eyes	15	15	
Age, years	67.5 ± 8.0	67.9 ± 7.5	0.90
Gender, male/female	4/11	4/11	1.00
BCVA-logMAR	-0.03 ± 0.10	0.80 ± 0.31	< 0.01
IOP, mmHg	13.9 ± 1.9	15.5 ± 2.6	0.051
SE, diopters	-0.26 ± 2.49	-0.42 ± 1.86	0.51
AL, mm	23.58 ± 0.98	23.65 ± 0.84	0.90
Duration of symptoms, month	-	1.80 ± 1.81	
HT, %	26.7	46.7	0.14
MH stage 2:3:4, eyes	-	4:7:4	
SBP, mmHg	126 ± 16	125 ± 11	0.76
DBP, mmHg	71 ± 11	75 ± 11	0.50
Retinal characteristics			
OCT parameter			
Minimum hole diameter, μm	-	331 ± 144	
Basal hole diameter, μm	-	676 ± 289	
Hole height, μm	-	434 ± 92	
EZ defect length, μm	-	1383 ± 409	
Indexes			
HFF	-	0.77 ± 0.16	
MHI	-	0.77 ± 0.38	
THI	-	1.50 ± 0.51	

IMH, idiopathic macular hole; BCVA, best-corrected visual acuity; IOP, intraocular pressure; SE, spherical equivalent; AL, axial length; HT, hypertension; SBP, systolic blood pressure; DBP, diastolic blood pressure; OCT, optical coherence tomography; EZ, ellipsoid zone; HFF, hole form factor; MHI, macular hole index; THI, tractional hole index

Statistically significant values are highlighted as bold

correlation coefficient (ICC) exceeded 0.9, proving high reliability. In addition, Bland–Altman plot was generated to determine the systematic bias (Fig. 3). To confirm the fixed bias, a 95% confidence interval was obtained for the mean of the differences between the two measurements. As shown in Table 2, there is no significant fixed bias in choroidal area and the L/C ratio in the control and IMH eyes. Next, to determine the proportional bias, the significance of the correlation between the measured and mean values of the corresponding two groups was tested. There was no significant proportional bias in choroidal area and L/C ratio in the control and IMH eyes. Overall, these data prove that there were no specific trends among the evaluators.

Analysis of choroidal structure in controls and IMH eyes

We investigated the difference between the choroidal binarization structure measurements of healthy control and the

preoperative IMH eye. Table 3 summarizes the structural features of the choroid. The CA, LA, and the L/C ratio in choriocapillaris of IMH eyes were significantly lower than those of control eyes, while SA was significantly greater in IMH than that in control eyes. In contrast, there was no significant difference in total choroid, Sattler's layer, Haller's layer, or CCT.

Correlation between retinal OCT parameters and choroidal structure

Table 4 shows the correlation between retinal OCT parameters and choroidal binarization structure in preoperative IMH eyes. MH stage showed a significant negative correlation with the L/C ratio in the total choroid and Haller's layer ($R = -0.68$, $P < 0.01$). Basal hole diameter showed a significant negative correlation with the L/C ratio in total choroid ($R = -0.66$, $P < 0.01$). The EZ defect length showed a significant negative correlation with the L/C ratio in total choroid and with CA and LA in the choriocapillaris ($R = -0.61$, $P < 0.05$, $R = -0.77$, $P < 0.01$, and $R = -0.71$, $P < 0.01$, respectively). HFF showed a significant negative correlation with the L/C ratio in the choriocapillaris ($R = -0.53$, $P < 0.05$). MHI and THI showed a significant positive correlation with the L/C ratio and CA in total choroid, respectively ($R = 0.57$, $P < 0.05$, and $R = 0.52$, $P < 0.05$, respectively). On the other hand, the correlation analysis also investigated the association between preoperative choroidal structural parameters and BCVA, but found no significant correlation (data not shown). We also examined the relationship between the choriocapillaris and the duration of ocular symptoms associated with IMH (1.80 ± 1.81 , month), but found no significant association (data not shown).

Changes in visual acuity, retinal, and choroidal structures after vitrectomy

After vitrectomy, MH was closed in all eyes. The mean BCVA at baseline, 1 month, and 2 months after surgery were 0.80 ± 0.31 , 0.51 ± 0.27 , and 0.45 ± 0.31 , respectively, and continued to improve over time ($P < 0.01$). LA and L/C ratio in the choriocapillaris showed an increase over time after surgery, and SA showed a decrease, which were statistically significant ($P < 0.05$, Table 5). The other choroidal layers did not show a consistent direction with respect to changes in choroidal structure. During the follow-up period up to 2 months after surgery, there was a statistically significant positive correlation between changes in BCVA and changes in EZ defect length (Fig. 4). On the other hand, no significant correlation was observed between the change in BCVA and the change in LA and the L/C ratio at choriocapillaris (data not shown).

Table 2 Inter-examiner reliability of choroidal segmentation for control and IMH eyes

		Relative reliability				Bland–Altman analysis				
						Fixed bias		Proportional bias		
		ICC (single)	<i>P</i> value	ICC (mean)	<i>P</i> value	CI 95%	<i>P</i> value	<i>R</i>	<i>P</i> value	
Control eyes	Choriocapillaris (CC)	CC area	0.9996	<0.01	0.9995	<0.01	–1003~1003	0.99	–0.21	0.49
		L/C ratio	0.9991	<0.01	0.9995	<0.01	–0.07~0.14	0.51	–0.36	0.18
	Sattler's layer (SL)	SL area	0.9892	<0.01	0.9946	<0.01	–4435~6053	0.75	0.16	0.56
		L/C ratio	0.9004	<0.01	0.9476	<0.01	–0.65~1.85	0.32	0.50	0.06
Haller's layer (HL)	HL area	0.9995	<0.01	0.9998	<0.01	–4718~6127	0.78	–0.21	0.46	
	L/C ratio	0.9978	<0.01	0.9989	<0.01	–0.12~0.18	0.72	0.20	0.48	
IMH eyes	Choriocapillaris (CC)	CC area	0.9818	<0.01	0.9908	<0.01	–1463~4019	0.33	0.13	0.66
		L/C ratio	0.9997	<0.01	0.9999	<0.01	–0.03~0.12	0.21	0.04	0.90
	Sattler's layer (SL)	SL area	0.9528	<0.01	0.9758	<0.01	–2225~7517	0.26	–0.29	0.31
		L/C ratio	0.9025	<0.01	0.9487	<0.01	–1.16~2.13	0.53	–0.06	0.84
	Haller's layer (HL)	HL area	0.9948	<0.01	0.9974	<0.01	–1636~9000	0.16	0.32	0.24
		L/C ratio	0.9896	<0.01	0.9948	<0.01	–0.34~0.36	0.96	0.09	0.74

IMH, idiopathic macular hole; ICC, intraclass coefficient; CI 95%, 95% confidence interval; L/C ratio, luminal/choroidal ratio

Discussion

This is the first study to evaluate the choroidal structure underlying the central foveal region of IMH patients before and after PPV by segmenting three vascular sublayers with using binarization technology [18, 19]. The major results showed that the vascular structure of the choriocapillaris before PPV was significantly reduced compared to that of healthy controls since CA, LA, and L/C ratio of the choriocapillaris in the IMH eyes was significantly lower than those of control eyes. The other sublayers, Sattler's and Haller's layers, however, had no significant difference. In addition, on comparing the pre-operative choriocapillaris area with the postoperative one, the latter showed to be significantly increased, indicating that the reduction in vascular structure of the choriocapillaris seen preoperatively improved after MH repair. This, therefore, implies that the morphological alteration may be a functional but not irreversible phenomenon in the choriocapillaris associated with the pathological condition of macular hole.

The choroid is composed primarily of blood vessels, which supply oxygen and nutrients to the outer retina and play an important role in maintaining normal metabolism of RPE and photoreceptors. Since EDI-OCT was introduced into various clinical researches, there has been accumulating evidence that the pathological condition of the choroid is associated with a variety of retinal diseases [25]. In fact, OCT showed that the choroidal thickness was reduced in IMH patients compared to healthy subjects [4]. Furthermore, OCTA to quantify choroidal circulation revealed

striking findings that choriocapillaris flow area and parafoveal vascular density in the macular region of IMH patients were significantly lower than in fellow eyes and healthy controls [26]. Gedik B et al. also with using OCTA investigated the choriocapillaris blood flow and described that the increase of the choriocapillaris blood flow after surgical repair of IMH continued up to 6 months postoperatively [27]. Thus, the alteration of choriocapillaris circulation around PPV was almost similar in a temporal sequence to the morphological changes observed in this study.

In addition to the choroidal vascular structure, this study further analyzed quantitatively MH configuration parameters including minimum hole diameter, basal hole diameter, and EZ defect length as well as the MH-related OCT indexes having correlation with postoperative visual acuity [22–24]. Tornambe PE proposed that macular hole progression is caused by instability of the underlying retina with progressive hydration of the retinal layers [28]. Nair U et al. used OCTA to investigate retinal micromorphology in IMH and showed a positive correlation between basal hole diameter and intraretinal cyst spaces [29]. The present study demonstrated that the EZ defect length showed a significant negative correlation with the L/C ratio in total choroid and with CA and LA in the choriocapillaris. Regarding the MH-related OCT indexes, HFF showed a significant negative correlation with the L/C ratio in the choriocapillaris. MHI and THI showed a significant positive correlation with the L/C ratio and CA in the total choroid. Results of the analysis among choroidal vascular structure, MH configuration parameters, and MH-related OCT indexes indicate that

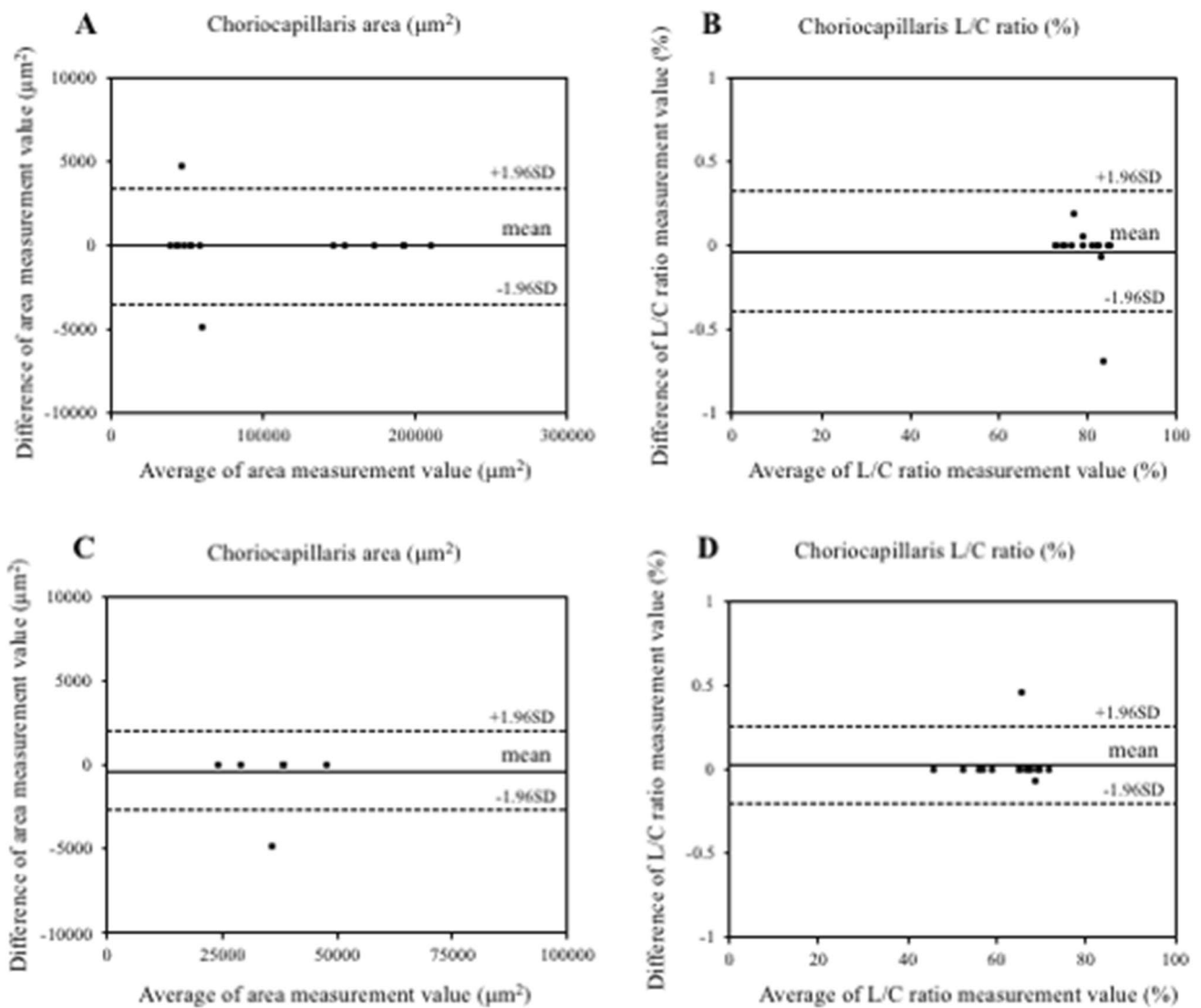


Fig. 3 Agreement between choriocapillaris area and luminal/choroidal area ratio (L/C ratio) using Bland–Altman plot. **A** Choriocapillaris area in control eyes. **B** Choriocapillaris L/C ratio in control eyes.

C Choriocapillaris area in idiopathic macular hole eyes. **D** Choriocapillaris L/C ratio idiopathic macular hole eyes

the anterior–posterior VMT and the retinal spaces could be correlated with the choriocapillaris vascular structures. Previous reports have shown that in the MH eye, localized retinal tissue defects disrupt microvascular structure and reduce the need for cellular metabolism [30]. Taken together, there is a mutualistic symbiotic relationship between components of the IMH-damaged photoreceptor/RPE/Bruch’s membrane/choriocapillaris complex, in which loss of this functionally integrated relationship can lead to dysfunction of all components within the complex. Therefore, the strong correlation between the EZ defect and the collapsed luminal area in the choriocapillaris vessels observed in this study may provide complementary evidence for the “hydration theory.”

Once MH is successfully closed following PPV, retinal vascular remodeling then occurs, accompanied by glial cell proliferation [31]. According to the hydration theory, surgery and gas tamponade make it impossible for vitreous fluid to continue to pass through the hole or penetrate the retina, isolating the liquefied vitreous from the MH [28]. At the same time, recontact of the sensory retina with RPE brings about physiological function of the photoreceptor/RPE/Bruch’s membrane/choriocapillaris complex. In addition, RPE cells continuously drain intraretinal cyst and subretinal fluid, eventually restoring the original macular structure. The present data indicate that the morphological recovery of choriocapillaris may contribute to the improvement of RPE pumping function. Wang et al. showed that laser-induced full-thickness MH

Table 3 Choroidal characteristics of control and IMH eyes

	Control eyes	IMH eyes	<i>P</i> value
Total choroid			
CA, × 10 ³ μm ²	423.1 ± 58.0	409.3 ± 105.8	0.55
LA, × 10 ³ μm ²	282.1 ± 46.0	267.2 ± 68.4	0.49
SA, × 10 ³ μm ²	140.9 ± 19.3	142.1 ± 39.4	0.95
L/C ratio, %	66.5 ± 3.6	65.3 ± 2.7	0.35
Choriocapillaris			
CA, × 10 ³ μm ²	47.3 ± 6.6	36.9 ± 6.2	< 0.01
LA, × 10 ³ μm ²	38.3 ± 5.6	23.4 ± 5.0	< 0.01
SA, × 10 ³ μm ²	9.0 ± 2.2	13.5 ± 2.9	< 0.01
L/C ratio, %	80.9 ± 4.1	63.1 ± 7.2	< 0.01
Sattler's layer			
CA, × 10 ³ μm ²	80.3 ± 21.8	94.5 ± 27.3	0.11
LA, × 10 ³ μm ²	52.1 ± 13.5	63.7 ± 17.2	0.06
SA, × 10 ³ μm ²	28.3 ± 10.4	30.9 ± 12.4	0.66
L/C ratio, %	65.4 ± 7.6	68.2 ± 6.6	0.44
Haller's layer			
CA, × 10 ³ μm ²	295.5 ± 46.4	277.9 ± 91.2	0.47
LA, × 10 ³ μm ²	191.8 ± 41.1	180.1 ± 59.3	0.52
SA, × 10 ³ μm ²	103.6 ± 14.3	97.8 ± 33.7	0.52
L/C ratio, %	64.4 ± 5.5	64.7 ± 4.3	0.82
CCT, μm	283 ± 38	274 ± 70	0.52

IMH, idiopathic macular hole; CA, choroidal area; LA, luminal area; SA, stromal area; L/C ratio, luminal/choroidal ratio, CCT, central choroidal thickness

Statistically significant values are highlighted as bold

can be treated by vitrectomy, but reported significantly poorer postoperative visual acuity in the group with RPE/choroidal damage compared to the group without RPE/choroidal damage [32]. Their OCTA also showed that choroidal ischemia caused by laser injury could involve inner choroidal levels, suggesting that the inner choroid of IMH eyes plays a critical role in the recovery of RPE and outer retinal functions following macular hole surgery. They described the possibility that the reduction in metabolic demands caused by the central retinal defect and the disruption of the anatomic structure of blood vessels due to parafoveal cysts could be improved by surgery, thereby provoking postoperative choriocapillaris blood flow. In this study, there was a correlation among basal hole diameter, EZ defect length, OCT parameters of HFF, MHI, and THI, and choroidal structures. In particular, we found a strong negative correlation between EZ defect length and luminal area in the choriocapillaris. In addition, LA and the L/C ratio in the choriocapillaris showed a significant increase after surgery. Therefore, changes in the choriocapillaris before and after PPV may reflect an improved balance

between supply and demand of oxygen that has collapsed due to temporary loss of central retinal function by MH.

From this, it is hypothesized that insufficient blood and oxygen supply associated with the decrease in choroidal blood vessels may increase the sensitivity to foveal traction depending on IMH formation and the stage progression. Aras et al. used a Heidelberg retinal flowmeter to measure foveal choriocapillaris blood flow and reported that stage Ia and stage 4 MH eyes had reduced foveal choroidal circulation compared to control eyes [3]. They suggested that IMH eyes are associated with decreased foveal choriocapillaris blood flow, although they were unable to assess the causal relationship of these findings to MH. Previous studies using laser speckle flowgraphy demonstrated that choroidal blood flow did not change before and after vitrectomy in IMH patients [33]. The 830 nm wavelength of the diode laser emitted from LSFG can penetrate deep into the choroid and has established its usefulness as an approach to perfusion measurement of larger choroidal vessels rather than choriocapillaris [34]. Although the authors cannot exclude the effect of choriocapillaris affecting the results, as mentioned above, the contribution of choriocapillaris blood flow by LSFG signal is much less than medium/large vessels. Thus, the effect of IMH on total choroidal circulation may be limited, so it is necessary to separate and evaluate the choroidal vascular layer.

The vascular branches feeding the macular choroid originate from short posterior ciliary arteries and penetrate the sclera to distribute into the choroid. Peripheral arterioles within the choroid are likely to supply blood to the choriocapillaris by forming the lobular pattern [35]. The blood then returns to the vein and flows into larger vessels to the ampulla of the vortex vein. Previously, we have studied the changes in choroidal thickness in diabetic macular edema eyes by splitting the inner and outer layers. We eventually found that the choroidal outer layer was significantly thickened in the group of DME patients who were not systemically treated for diabetes mellitus and that systemic status preferentially affects the choroidal “outer layer” thickness [36]. On the other hand, the systemic status of the IMH patients examined in this study did not differ from that of the controls; therefore, we speculate that the photoreceptor/RPE/Bruch's membrane/choriocapillaris complex was affected by topical treatments including vitrectomy rather than larger choroidal vascular structures.

The choriocapillaris vasculatures as well as photoreceptor structure together with BCVA significantly improved 2 months after PPV in the present study. On the other hand, there was no significant correlation between choriocapillaris vasculatures and postoperative BCVA. A

Table 4 Spearman correlation coefficient matrix for retinal OCT parameter and choroidal structure in IMH eyes

	MH stage		Minimum hole diameter		Basal hole diameter		EZ defect length		HFF		MHI		THI	
	<i>R</i>	<i>P</i> value	<i>R</i>	<i>P</i> value	<i>R</i>	<i>P</i> value	<i>R</i>	<i>P</i> value	<i>R</i>	<i>P</i> value	<i>R</i>	<i>P</i> value	<i>R</i>	<i>P</i> value
Total choroid														
CA	−0.23	0.40	−0.25	0.37	−0.10	0.73	−0.17	0.55	0.35	0.20	0.17	0.55	0.52	< 0.05
LA	−0.36	0.19	−0.28	0.31	−0.19	0.49	−0.27	0.33	0.30	0.27	0.21	0.46	0.48	0.07
SA	−0.09	0.76	−0.12	0.66	0.06	0.82	−0.04	0.89	0.26	0.35	0.03	0.92	0.39	0.16
L/C ratio	−0.68	< 0.01	−0.35	0.21	−0.66	< 0.01	−0.61	< 0.05	0.06	0.83	0.57	< 0.05	0.22	0.43
Choriocapillaris														
CA	−0.35	0.21	−0.28	0.31	−0.50	0.06	−0.77	< 0.01	0.17	0.54	0.42	0.12	0.16	0.57
LA	−0.32	0.25	−0.27	0.33	−0.40	0.14	−0.71	< 0.01	−0.07	0.81	0.29	0.29	0.09	0.75
SA	−0.13	0.65	−0.07	0.80	−0.26	0.35	−0.27	0.33	0.46	0.08	0.32	0.25	0.13	0.65
L/C ratio	−0.21	0.45	−0.05	0.86	−0.10	0.73	−0.39	0.15	−0.53	< 0.05	−0.02	0.94	−0.20	0.47
Sattler's layer														
CA	−0.49	0.07	−0.46	0.08	−0.26	0.34	−0.31	0.26	0.00	0.99	0.25	0.37	0.31	0.26
LA	−0.40	0.14	−0.49	0.07	−0.26	0.34	−0.32	0.24	0.09	0.74	0.29	0.29	0.33	0.23
SA	−0.30	0.28	−0.18	0.52	0.06	0.83	−0.06	0.82	−0.13	0.66	−0.08	0.79	0.16	0.57
L/C ratio	0.21	0.45	−0.15	0.58	−0.24	0.38	−0.20	0.47	0.24	0.39	0.33	0.23	0.10	0.73
Haller's layer														
CA	−0.11	0.71	−0.06	0.83	0.04	0.90	−0.04	0.89	0.25	0.36	0.03	0.93	0.36	0.19
LA	−0.19	0.50	−0.16	0.56	−0.08	0.77	−0.13	0.66	0.31	0.26	0.13	0.64	0.44	0.10
SA	0.02	0.94	−0.04	0.89	0.12	0.68	0.01	0.96	0.32	0.24	−0.01	0.98	0.36	0.19
L/C ratio	−0.57	< 0.05	−0.01	0.96	−0.29	0.30	−0.29	0.30	−0.16	0.57	0.15	0.60	−0.08	0.79

OCT, optical coherence tomography; IMH, idiopathic macular hole; EZ, ellipsoid zone; HFF, hole form factor; MHI, macular hole index; THI, tractional hole index; CA, choroidal area; LA, luminal area; SA, stromal area; L/C ratio, luminal/choroidal ratio

Statistically significant values are highlighted as bold

structurally and functionally normal choroidal vasculature is essential for retinal function, and abnormal choroidal blood volume and/or impaired blood flow can result in photoreceptor and RPE dysfunction and in subsequent death. However, recovery of macular function after MH closure is not always completed within 2 months, and the same thing can be applied for the choroid. Teng et al. showed that the choriocapillaris flow area and density increased significantly 1 month after vitrectomy for IMH eyes, but not significantly correlated with visual acuity [26]. Previously, we observed changes in choroidal structure before and after treatment for eyes with diabetic macular edema and reported that high pretreatment L/C ratio showed a significant inverse correlation with good visual acuity after 24 months [12]. In other words, we speculated that a higher L/C ratio could restore normal choroidal vascular components and maintain choroidal circulation and metabolism of the outer retinal layer. Therefore, a longer follow-up period is needed to verify whether increased choriocapillaris circulation after MH surgery contributes to improvements of visual acuity.

Limitation

Although the strength of this study was to demonstrate alterations of choroidal vascular structures in IMH, there are some limitations to note in our study. First, the sample size of enrolled patients was relatively small. Further researches with a larger sample size are needed to ensure the results. Second, the follow-up period was relatively short; being two months after surgery. The current study showed improvement in choroidal vascular structures after surgery, but no correlation with improved visual acuity based on short-term observations. Long-term follow-up studies are needed to better understand relationships with each other. Third, there are some biases associated with imaging technology of EDI-OCT, where deep signal capture depends on the characteristics of the overlying tissue. Therefore, future studies will also prove the difference between EDI-OCT and SS-OCT data in IMH eyes. Fourth, since it remains unclear whether the structural changes in the choriocapillaris observed after vitrectomy are specific to IMH repair, further investigations on the changes of choroidal structures in vitrectomised eyes with other etiologies are needed.

Table 5 Postoperative changes in choroidal structure in IMH eyes

	Pre	Post		Friedman test (<i>P</i> value)	Scheffe's paired comparison (<i>P</i> value)		
		1 M	2 M		Pre—1 M	Pre—2 M	1 M—2 M
Total choroid							
CA, × 10 ³ μm ²	409.3 ± 105.8	423.7 ± 119.1	423.5 ± 121.7	0.44	NA	NA	NA
LA, × 10 ³ μm ²	267.2 ± 68.4	285.1 ± 75.7	287.0 ± 78.1	0.08	NA	NA	NA
SA, × 10 ³ μm ²	142.1 ± 39.4	138.7 ± 45.8	136.5 ± 44.9	0.82	NA	NA	NA
L/C ratio, %	65.3 ± 2.7	67.6 ± 2.5	68.0 ± 2.2	0.17	NA	NA	NA
Choriocapillaris							
CA, × 10 ³ μm ²	36.9 ± 6.2	37.4 ± 4.7	40.3 ± 4.9	0.09	NA	NA	NA
LA, × 10 ³ μm ²	23.4 ± 5.0	27.7 ± 3.8	30.9 ± 4.4	< 0.01	0.19	< 0.01	0.19
SA, × 10 ³ μm ²	13.5 ± 2.9	9.7 ± 3.1	9.4 ± 2.4	< 0.01	< 0.01	< 0.01	0.98
L/C ratio, %	63.1 ± 7.2	74.3 ± 6.4	76.6 ± 5.4	< 0.01	< 0.01	< 0.01	0.44
Sattler's layer							
CA, × 10 ³ μm ²	94.5 ± 27.3	93.9 ± 19.4	95.1 ± 24.1	0.94	NA	NA	NA
LA, × 10 ³ μm ²	63.7 ± 17.2	64.2 ± 14.9	65.4 ± 15.6	0.94	NA	NA	NA
SA, × 10 ³ μm ²	30.9 ± 12.4	29.7 ± 8.1	29.7 ± 10.1	0.63	NA	NA	NA
L/C ratio, %	68.2 ± 6.6	68.6 ± 7.0	69.5 ± 5.8	0.77	NA	NA	NA
Haller's layer							
CA, × 10 ³ μm ²	277.9 ± 91.2	292.5 ± 107.7	288.1 ± 104.2	0.42	NA	NA	NA
LA, × 10 ³ μm ²	180.1 ± 59.3	193.2 ± 68.6	190.7 ± 66.6	0.19	NA	NA	NA
SA, × 10 ³ μm ²	97.8 ± 33.7	99.3 ± 40.9	97.4 ± 38.4	1.00	NA	NA	NA
L/C ratio, %	64.7 ± 4.3	66.3 ± 3.1	66.3 ± 2.9	0.63	NA	NA	NA

IMH, idiopathic macular hole; M, month; CA, choroidal area; LA, luminal area; SA, stromal area; L/C ratio, luminal/choroidal ratio; NA, not applicable

Statistically significant values are highlighted as bold

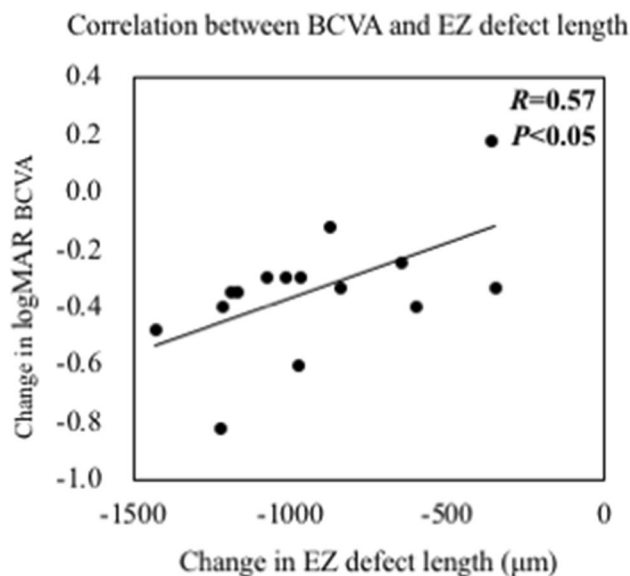


Fig. 4 Correlation between best-corrected visual acuity (BCVA) and ellipsoid zone (EZ) defect length at choriocapillaris in idiopathic macular hole. Correlation was investigated using Spearman's rank correlation coefficient

Conclusion

Our study demonstrates that changes in choroidal vascular structures in IMH exclusively took place in the choriocapillaris, and that it recovers after MH repair. Furthermore, we found that this change in the choriocapillaris may correlate with a reversible disruption in photoreceptor layer structure. Morphological defects in the macular retina may temporarily reduce the need for local blood supply and alter choroidal vascular structures.

Declarations

Ethical approval This study followed the principles of the Declaration of Helsinki. Institutional review board in Teine Keijinkai Hospital (IRB number: 2–021372-00) approved this study.

Research involving human participants and/or animals This study involves human participants with retrospective, non-invasive observations.

Informed consent For this type of study, formal consent is not required.

Conflict of interest The authors declare no competing interests.

References

1. Gass JDM (1988) Idiopathic senile macular hole. Its early stages and pathogenesis. *Arch Ophthalmol* 106:629–639. <https://doi.org/10.1001/ARCHOPHT.1988.01060130683026>
2. Johnson RN, Gass JDM (1988) Idiopathic macular holes. Observations, stages of formation, and implications for surgical intervention. *Ophthalmology* 95:917–924. [https://doi.org/10.1016/S0161-6420\(88\)33075-7](https://doi.org/10.1016/S0161-6420(88)33075-7)
3. Aras C, Ocakoglu O, Akova N (2004) Foveolar choroidal blood flow in idiopathic macular hole. *Int Ophthalmol* 25:225–232. <https://doi.org/10.1007/S10792-005-5014-4>
4. Zhang P, Zhou M, Wu Y et al (2017) CHOROIDAL thickness in unilateral idiopathic macular hole: a cross-sectional study and meta-analysis. *Retina* 37:60–69. <https://doi.org/10.1097/IAE.0000000000001118>
5. Pichi F, Aggarwal K, Neri P et al (2018) Choroidal biomarkers. *Indian J Ophthalmol* 66:1716–1726. https://doi.org/10.4103/IJO.IJO_893_18
6. Sonoda S, Sakamoto T, Yamashita T et al (2015) Luminal and stromal areas of choroid determined by binarization method of optical coherence tomographic images. *Am J Ophthalmol* 159:1123–1131.e1. <https://doi.org/10.1016/j.ajo.2015.03.005>
7. Agrawal R, Gupta P, Tan KA, et al (2016) Choroidal vascularity index as a measure of vascular status of the choroid: Measurements in healthy eyes from a population-based study. *Sci Rep* 6 <https://doi.org/10.1038/SREP21090>
8. Sonoda S, Sakamoto T, Kuroiwa N, et al (2016) Structural changes of inner and outer choroid in central serous chorioretinopathy determined by optical coherence tomography. *PLoS One* 11 <https://doi.org/10.1371/JOURNAL.PONE.0157190>
9. Ting DSW, Yanagi Y, Agrawal R, et al (2017) Choroidal remodeling in age-related macular degeneration and polypoidal choroidal vasculopathy: a 12-month prospective study. *Sci Rep* 7 <https://doi.org/10.1038/S41598-017-08276-4>
10. Ng WY, Ting DSW, Agrawal R et al (2016) Choroidal structural changes in myopic choroidal neovascularization after treatment with anti-vascular endothelial growth factor over 1 year. *Invest Ophthalmol Vis Sci* 57:4933–4939. <https://doi.org/10.1167/IOVS.16-20191>
11. Kase S, Endo H, Takahashi M et al (2020) Alteration of choroidal vascular structure in diabetic retinopathy. *Br J Ophthalmol* 104:417–421. <https://doi.org/10.1136/BJOPHTHALMOL-2019-314273>
12. Kase S, Endo H, Takahashi M et al (2022) Involvements of choroidal vascular structures with local treatments in patients with diabetic macular edema. *Eur J Ophthalmol* 32:450–459. <https://doi.org/10.1177/11206721211027103>
13. Kase S, Endo H, Takahashi M et al (2021) Choroidal vascular structures in diabetic patients: a meta-analysis. *Graefes Arch Clin Exp Ophthalmol* 259:3537–3548. <https://doi.org/10.1007/S00417-021-05292-Z>
14. Mitamura Y, Enkhmaa T, Sano H et al (2021) Changes in choroidal structure following intravitreal aflibercept therapy for retinal vein occlusion. *Br J Ophthalmol* 105:704–710. <https://doi.org/10.1136/BJOPHTHALMOL-2020-316214>
15. Kawano H, Sonoda S, Yamashita T et al (2016) Relative changes in luminal and stromal areas of choroid determined by binarization of EDI-OCT images in eyes with Vogt-Koyanagi-Harada disease after treatment. *Graefes Arch Clin Exp Ophthalmol* 254:421–426. <https://doi.org/10.1007/S00417-016-3283-4>
16. Egawa M, Mitamura Y, Niki M et al (2019) Correlations between choroidal structures and visual functions in eyes with retinitis pigmentosa. *Retina* 39:2399–2409. <https://doi.org/10.1097/IAE.0000000000002285>
17. Chun H, Kim JY, Kwak JH, et al (2021) The effect of phacoemulsification performed with vitrectomy on choroidal vascularity index in eyes with vitreomacular diseases. *Sci Rep* 11 <https://doi.org/10.1038/S41598-021-99440-4>
18. Sonoda S, Sakamoto T, Kakiuchi N et al (2018) Semi-automated software to measure luminal and stromal areas of choroid in optical coherence tomographic images. *Jpn J Ophthalmol* 62:179–185. <https://doi.org/10.1007/S10384-017-0558-1>
19. Sonoda S, Terasaki H, Kakiuchi N et al (2019) Kago-Eye2 software for semi-automated segmentation of subfoveal choroid of optical coherence tomographic images. *Jpn J Ophthalmol* 63:82–89. <https://doi.org/10.1007/S10384-018-0631-4>
20. Kinoshita T, Mitamura Y, Mori T, et al (2016) Changes in choroidal structures in eyes with chronic central serous chorioretinopathy after half-dose photodynamic therapy. *PLoS One* 11 <https://doi.org/10.1371/JOURNAL.PONE.0163104>
21. Endo H, Kase S, Takahashi M et al (2018) Alteration of layer thickness in the choroid of diabetic patients. *Clin Exp Ophthalmol* 46:926–933. <https://doi.org/10.1111/CEO.13299>
22. Ullrich S, Haritoglou C, Gass C et al (2002) Macular hole size as a prognostic factor in macular hole surgery. *Br J Ophthalmol* 86:390–393. <https://doi.org/10.1136/BJO.86.4.390>
23. Kusuhara S, Teraoka Escaño MF, Fujii S et al (2004) Prediction of postoperative visual outcome based on hole configuration by optical coherence tomography in eyes with idiopathic macular holes. *Am J Ophthalmol* 138:709–716. <https://doi.org/10.1016/j.ajo.2004.04.063>
24. Ruiz-Moreno JM, Staicu C, Piñero DP et al (2008) Optical coherence tomography predictive factors for macular hole surgery outcome. *Br J Ophthalmol* 92:640–644. <https://doi.org/10.1136/BJO.2007.136176>
25. Laviers H, Zambarakji H (2014) Enhanced depth imaging-OCT of the choroid: a review of the current literature. *Graefes Arch Clin Exp Ophthalmol* 252:1871–1883. <https://doi.org/10.1007/S00417-014-2840-Y>
26. Teng Y, Yu M, Wang Y et al (2017) OCT angiography quantifying choriocapillary circulation in idiopathic macular hole before and after surgery. *Graefes Arch Clin Exp Ophthalmol* 255:893–902. <https://doi.org/10.1007/S00417-017-3586-0>
27. Gedik B, Suren E, Bulut M, et al (2021) Changes in choroidal blood flow in patients with macular hole after surgery. *Photodiagnosis Photodyn Ther* 35 <https://doi.org/10.1016/j.pdpdt.2021.102428>
28. Tornambe PE (2003) Macular hole genesis: the hydration theory. *Retina* 23:421–424. <https://doi.org/10.1097/00006982-200306000-00028>
29. Nair U, Sheth JU, Indurkar A, Soman M (2021) Intraretinal cysts in macular hole: a structure-function correlation based on en face imaging. *Clin Ophthalmol* 15:2953–2962. <https://doi.org/10.2147/OPHTH.S321594>
30. Sano M, Shimoda Y, Hashimoto H, Kishi S (2009) Restored photoreceptor outer segment and visual recovery after macular hole closure. *Am J Ophthalmol* 147 <https://doi.org/10.1016/j.ajo.2008.08.002>
31. Michalewska Z, Michalewski J, Adelman RA, Nawrocki J (2010) Inverted internal limiting membrane flap technique for large macular holes. *Ophthalmology* 117:2018–2025. <https://doi.org/10.1016/j.opthta.2010.02.011>
32. Wang X, Zhang T, Jiang R, Xu G (2021) Vitrectomy for laser-induced full-thickness macular hole. *BMC Ophthalmol* 21 <https://doi.org/10.1186/S12886-021-01893-8>
33. Okamoto M, Matsuura T, Ogata N (2014) Ocular blood flow before, during, and after vitrectomy determined by laser speckle flowgraphy. *Ophthalmic Surg Lasers Imaging Retina* 45:118–124. <https://doi.org/10.3928/23258160-20140306-04>

34. Hashimoto Y, Saito W, Saito M et al (2015) Decreased choroidal blood flow velocity in the pathogenesis of multiple evanescent white dot syndrome. *Graefes Arch Clin Exp Ophthalmol* 253:1457–1464. <https://doi.org/10.1007/S00417-014-2831-Z>
35. Hanyuda N, Akiyama H, Shimoda Y et al (2017) Different filling patterns of the choriocapillaris in fluorescein and indocyanine green angiography in primate eyes under elevated intraocular pressure. *Invest Ophthalmol Vis Sci* 58:5856–5861. <https://doi.org/10.1167/IOVS.17-22223>
36. Endo H, Kase S, Takahashi M, et al (2020) Relationship between diabetic macular edema and choroidal layer thickness. *PLoS One* 15 <https://doi.org/10.1371/JOURNAL.PONE.0226630>

Publisher's note Springer Nature remains neutral with regard to jurisdictional claims in published maps and institutional affiliations.

Springer Nature or its licensor (e.g. a society or other partner) holds exclusive rights to this article under a publishing agreement with the author(s) or other rightsholder(s); author self-archiving of the accepted manuscript version of this article is solely governed by the terms of such publishing agreement and applicable law.